Quantification of unimolecular photoreaction kinetics. Determination of quantum yields and development of actinometers.

The photodegradation case of cardiovascular drug Nisoldipine.

Mounir Maafi, Wassila Maafi*

Leicester School of Pharmacy, De Montfort University, The Gateway, Leicester LE1 9BH, UK

Keywords: Nisoldipine, Φ–order photokinetics, photodegradation, spectrokinetics, quantum yield, self photostabilisation, dye effects, actinometry.

Corresponding Author
*E-mail: mmaafi@dmu.ac.uk; Tel.: +44 116 257 7704; fax: +44 116 257 7287.

Abstract

The lack of integrated rate-laws for photoreactions has led to carry out the treatment of drugs photodegradation kinetic data using the classical zeroth-, first- and second-order kinetics that were originally developed for thermal reactions. The recent developments of Φ–order kinetic models has opened new perspectives in the treatment of photoreaction kinetics of systems involving a photolabile molecule (A) transforming into a photochemically and thermally stable product (B), i.e. the AB(1Φ) photoreaction systems. Within this framework, the kinetics of cardiovascular and photosensitive drug Nisoldipine (*NIS*) has been rationalised. Continuous and monochromatic irradiation of *NIS* in ethanol obeyed Φ–order kinetics with a sigmoid–shaped quantum yield variation with irradiation wavelength (0.0041–0.35 within 235–390 nm spectral region). Both *NIS* initial concentration-induced self photostabilisation effect and the photostabilisation by absorption competitors were quantified (up 70 %) and related to a reduction of the photokinetic factor. Finally, the Φ–order kinetics also served to demonstrate the actinometric potential of *NIS* for the 320–400 nm dynamic range.

1. Introduction

Φ–order kinetics is a recently developed approach useful for the investigation and characterisation of unimolecular and reversible photodegradation reactions of drugs (1-7). It has been proven to be more suitable for the description of drugs' photoreactivity than the classical treatments based on zeroth, first and second reaction orders (1-4). In this respect, Φ–order kinetics palliate the main drawbacks of the classical strategy in four aspects: (i)– its equations are based on the differential equations of photo– and not thermal reactions, (ii)– it allows achieving a unique interpretation of the experimental data of reaction kinetic profiles conversely to the thermal strategy that may lead to ambiguity on the true order obeyed by the photoreaction studied, (iii)– it applies to the whole set of data making up the kinetic trace of the phototransformation and is not limited to a partial section (usually up to the half-life time) of the trace, and (iv)– it provides an analytical expression for the reaction rate–constant that refines the physical meaning of this parameter for such photoreactions. As such, Φ–order kinetics may serve to amend the ICH recommendations by introducing procedures and standard kinetic data treatment methods for the quantification of drugs' photodegradation kinetics that are lacking in the Q1b document relative to the photostability of drugs (8).

Nisoldipine (*NIS*), ((±)3–isobutyl–5–methyl–1,4–dihydro–2,6-dimethyl–4–(2–nitrophenyl)–pyridine–3,5–dicarboxylate), is a member of the 1,4–dihydropyridine class of calcium channel antagonist drugs. *NIS* is prescribed for the treatment of hypertension and angina (9).

The presence of a nitro group at the *ortho* position of the phenyl ring in some members of the 1,4–dihydropyridines such as *NIS* and nifedipine makes them particularly prone to photolability. The photodegradation mechanism of *NIS* (Scheme 1) involves an oxidation of the dihyropyridine

moiety to a pyridine ring and the reduction of the aromatic nitro group to a nitroso (9). This change in chemical structure results in a significant loss of therapeutic efficacy (10). As a consequence, a number of studies have been devoted to the study of the photodegradation of *NIS* under various conditions.

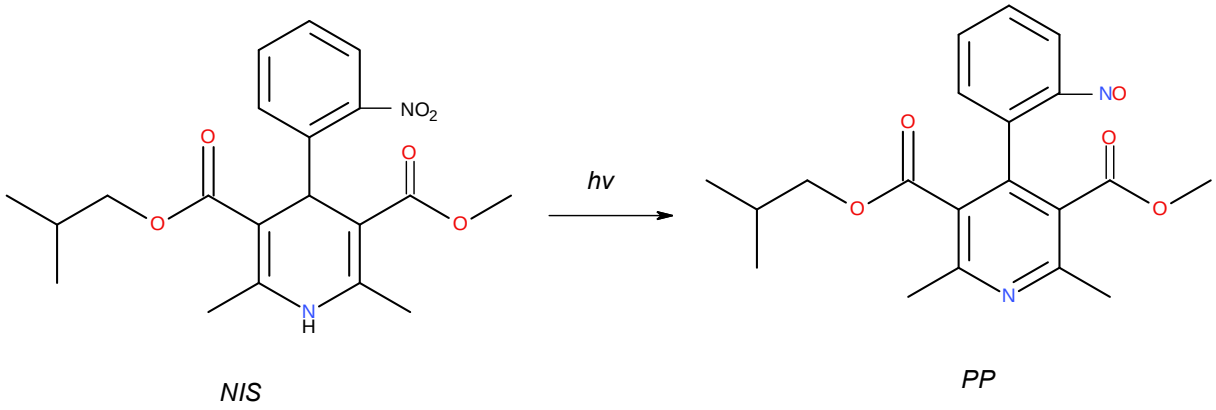

NIS *PP*

Scheme 1. *Nisoldipine (NIS) unimolecular and light induced transformation.*

Although much effort has been devoted to the elucidation of the photo–decomposition products of *NIS*, studies on the kinetics of its photodegradation remain scarce and largely controversial. For instance, the photoconversion of *NIS* in methanolic solutions using UV spectrophotometry and RP–HPLC was attributed a first–order kinetics (11), whereas another similar spectrophotometric study in ethanol described *NIS* kinetics by an apparent first–order up to a concentration of $3x10^{-5}$ M and the zero–order for concentrations higher than $2x10^{-4}$ M (12). In the solid state, *NIS* photodegradation monitored by HPLC, was ascribed a zero–order kinetics under daylight but the reaction order could not be clearly identified under UV illumination. In the latter case, *NIS* degradation showed a more complicated kinetic behaviour whereby the decrease of its concentration was linear with time up to *ca.* 60% of the initial concentration then it followed a much slower regime (13). However, the primary photoprocess of *NIS* degradation in solution leads

77 to a unique photoproduct: the nitroso derivative, *PP* in Scheme 1 (9, 14, 15) and any minor
78 products that might be detected in the reactive medium (10) must result from further slow thermal
79 degradation of *PP* (14).

80

81 The aim of this paper is to conduct a full elucidation of *NIS* kinetics in ethanol using Φ–order
82 kinetics. The irradiation–dependent quantum yields will be determined and the effects of initial
83 concentration and absorption competitors quantified. Finally, the potential use of *NIS* in
84 actinometry will be demonstrated.

85

86

87

88

2. Materials and methods

2.1.Materials

Nisoldipine (*NIS*), ((±)3-isobutyl-5-methyl-1,4-dihydro-2,6-dimethyl-4-(2-nitrophenyl)-pyridine-3,5-dicarboxylate), tartrazine (*TRZ*), quinoline yellow (*QY*) and spectroscopic grade ethanol were purchased from Aldrich and were used without further purification.

2.2.Monochromatic continuous irradiation

For irradiation experiments, a Ushio 1000 W xenon arc-lamp light source housed in a housing shell model A6000 and powered by a power supply model LPS–1200, was used. This setting was cooled by tap water circulation through a pipe system. The lamp housing was connected to a monochromator model 101 that allows the selection of specific irradiation wavelenghths since it consists of a special f/2.5 monochromator with a 1200 groove/mm at 300 nm blaze grating. The excitation beam was guided through an optical fibre to impinge from the top of the sample cuvette i.e. the excitation and the analysis light beams were perpendicular to each other. The set up was manufactured by Photon Technology International Corporation.

2.3.The monitoring system

A diode array spectrophotometer (Agilent 8453) was used to measure the various absorption spectra and kinetic profiles for the irradiation and calibration experiments. This spectrophotometer was equipped with a 1-cm cuvette sample holder and a Peltier system model Agilent 8453 for temperature control. As such, the sample was kept at 22°C, stirred continuously during the

112 experiment, and completely shielded from ambient light. The spectrophotometer was monitored by
113 an Agilent 8453 Chemstation kinetics–software.

114

115 A Radiant Power/Energy meter model 70260 was used to measure the radiant power of the incident
116 excitation beams.

117

118 *2.4.Kinetic data treatment*

119 In order to carry out non–linear fittings and to determine best-fit curves, a Levenberg-Marquardt
120 iterative program within the Origin 6.0 software was used.

121

122 *2.5.Solutions*

123 A 4.9 x 10^{-4} M stock solution of *NIS* in ethanol was prepared by weighing the solid. The stock
124 solution was diluted to prepare fresh analytical solutions (*ca*. 7.8 x 10^{-6} M) for analysis of
125 irradiation experiments performed at various wavelengths.

126

127 Since *NIS* absorbs in the UV and visible regions of the spectrum, particular care was taken during
128 the handling of *NIS* solutions using aluminium foil paper wrapping and keeping them in the fridge
129 while not in use. As such, *NIS* stock solutions remained stable for several weeks.

130

131 Stock solutions of *TRZ* (9.14 x 10^{-5} M) and *QY* (6.17 x 10^{-5} M) were prepared in ethanol from their
132 respective powders. Diluted solutions of the dyes in ethanol were then spiked with volumes from
133 *NIS* stock to make up solutions of the required concentrations.

134

135 *TRZ* and *QY* were selected since their spectrum largely overlaps that of *NIS* and could therefore act
136 as competitive absorbers of irradiation. Photoprotection experiments were conducted in quartz
137 cuvettes. The spectrum of the dye solution (of known concentration) was taken before this solution
138 was used for a blank experiment. Subsequently, a specific volume (a few μL) of *NIS* stock solution
139 was added to the dye solution. Thus, it was possible to record only the UV/Vis spectra of the
140 reactive medium (*NIS* and *PP*) during the reaction progress (with the measurement not being
141 hampered by the absorbance of the dye, present in the medium).

142

143 For actinometric studies, *NIS* ethanolic solutions of the same concentrations (*ca*. 7 x 10^{-6} M) were
144 exposed to specific irradiation wavelengths using a series of different intensities for each
145 wavelength. The kinetic traces were observed at an observation wavelength of 390 nm and were
146 subsequently fitted with the Φ–order equations.

147

148 Experiments were conducted at least in triplicates.

149

3. Theoretical basis

3.1. The Φ–order semi–empirical integrated rate–law for AB(1Φ) systems

The general semi–empirical integrated rate–law equation describing the time variation of the cumulative absorbance of the reactive medium involving the phototransformation of *NIS* into its photoproduct (*PP*) (Scheme 1) is given by the logarithmic Eq.1 (3). This type of reactions involving a single photochemical step ($\Phi_{A\rightarrow B}^{\lambda_{irr}}$) between the initial species (A) and its photoproduct (B) are generally labelled AB(1Φ) systems. The formula of Eq.1 has been established considering that the solution, subjected to a monochromatic, non-isosbestic and continuous irradiation (λ_{irr}), is homogeneously and continuously stirred. It is also assumed that the concentration of the excited–state species is negligible, the medium temperature is constant, and at the irradiation wavelength (λ_{irr}), species *NIS* and *PP* may absorb different amounts of light ($P_{\lambda_{irr}}$), i.e. the absorption coefficients of the species may be different ($\varepsilon_{NIS}^{\lambda_{irr}} \neq \varepsilon_{PP}^{\lambda_{irr}} \neq 0$).

$$A_{tot}^{\lambda_{irr}/\lambda_{obs}}(t) = A_{PP}^{\lambda_{irr}/\lambda_{obs}}(\infty) + \frac{A_{NIS}^{\lambda_{irr}/\lambda_{obs}}(0) - A_{PP}^{\lambda_{irr}/\lambda_{obs}}(\infty)}{A_{NIS}^{\lambda_{irr}/\lambda_{irr}}(0) - A_{PP}^{\lambda_{irr}/\lambda_{irr}}(\infty)} \times \frac{l_{\lambda_{obs}}}{l_{\lambda_{irr}}} \times Log\left[1 + \left(10^{-\left[\left(A_{NIS}^{\lambda_{irr}/\lambda_{irr}}(0) - A_{PP}^{\lambda_{irr}/\lambda_{irr}}(\infty)\right) \times \frac{l_{\lambda_{irr}}}{l_{\lambda_{obs}}}\right]} - 1\right) \times e^{-k_{NIS}^{\lambda_{irr}} \times t}\right] \quad (1)$$

with $l_{\lambda_{irr}}$ being the optical path length of the irradiation beam inside the sample and $l_{\lambda_{obs}}$ is the optical path length of the spectrophotometer monitoring light. The absorbances ($A^{\lambda\ /\lambda}$) in Eq.1 correspond to the observed measurements by the instrument (i.e. along $l_{\lambda_{obs}}$) of the reactive medium, at a given reaction time ($A_{tot}^{\lambda_{irr}/\lambda_{obs}}(t)$), at the initial time (t=0, $A_{NIS}^{\lambda_{irr}/\lambda_{obs}}(0)$ and $A_{NIS}^{\lambda_{irr}/\lambda_{irr}}(0)$), and at the end of the reaction (t = ∞ , $A_{PP}^{\lambda_{irr}/\lambda_{obs}}(\infty)$ and $A_{PP}^{\lambda_{irr}/\lambda_{irr}}(\infty)$ where only the photoproduct is present). The absorbances can be read out from the spectra at the particular wavelengths of irradiation (λ_{irr}) and observation (λ_{obs}) which might or not be the same. Therefore, each absorbance is dually labelled by the irradiation and the observation wavelengths ($\lambda_{irr}/\lambda_{irr}$ or $\lambda_{irr}/\lambda_{obs}$) corresponding to the specific measurement.

The exponential factor in Eq.1, $k_{NIS}^{\lambda_{irr}}$, represents the overall photoreaction rate–constant, that can be analytically expressed as;

$$k_{NIS}^{\lambda_{irr}} = \Phi_{NIS\rightarrow PP}^{\lambda_{irr}} \times \varepsilon_{NIS}^{\lambda_{irr}} \times l_{\lambda_{irr}} \times F_{\infty}^{\lambda_{irr}} \times P_{\lambda_{irr}} = \beta_{\lambda_{irr}} \times P_{\lambda_{irr}} \qquad (2)$$

where $\Phi_{NIS\rightarrow PP}^{\lambda_{irr}}$ is the quantum yield of *NIS* photoconversion, realised at the non–isosbestic irradiation wavelength (λ_{irr}), $\varepsilon_{NIS}^{\lambda_{irr}}$ is the molar absorption coefficient of *NIS*, $P_{\lambda_{irr}}$ is the radiant power, and $F_{\infty}^{\lambda_{irr}}$ the photokinetic factor expressed as;

$$F_{\infty}^{\lambda_{irr}} = \frac{1 - 10^{-\left(A_{tot}^{\lambda_{irr}/\lambda_{irr}}(\infty) \times \frac{l_{\lambda_{irr}}}{l_{\lambda_{obs}}}\right)}}{A_{tot}^{\lambda_{irr}/\lambda_{irr}}(\infty) \times \frac{l_{\lambda_{irr}}}{l_{\lambda_{obs}}}} \quad (3)$$

It is worth noting that in the case where another absorbing species is present in the reactive medium with *NIS* without being itself photoactive, such as a pharmaceutical excipient, the formula of the photokinetic factor (Eq.3) must be amended to take into account the effect of such an exogenous absorbing species. This is implemented by considering that the total absorbance of the medium at reaction completion includes both *PP* ($A_{PP}^{\lambda_{irr}/\lambda_{irr}}(\infty)$) and excipient ($A_{Excip.}^{\lambda_{irr}}$) absorbances, i.e. $A_{tot}^{\lambda_{irr}/\lambda_{irr}}(\infty) = A_{PP}^{\lambda_{irr}/\lambda_{irr}}(\infty) + A_{Excip.}^{\lambda_{irr}}$, instead of being only equal to that of PP, $A_{tot}^{\lambda_{irr}/\lambda_{irr}}(\infty) = A_{PP}^{\lambda_{irr}/\lambda_{irr}}(\infty)$, as is the case in the absence of excipient (3).

The aforementioned equations (Eqs. 1–3) have been validated by testing their reliability to fit synthetic data for AB(1Φ) systems that have been generated by Runge–Kutta numerical integration method. The optimization of these equations was realised by considering a large number of reactions including a wide range of reaction attributes and experimental conditions (3). The development of this semi–empirical framework was meant to circumvent the impossibility to achieve a closed–form integration of the photoreaction differential equation when both initial species and photoproduct absorb. The expression previously established for the photodegradation of the initial species as the only absorbing species ($\varepsilon_B^{\lambda_{irr}} = 0$) (1), represented a template for the derivation of Eq.1. In fact, the formulae for the latter case can be retrieved from Eqs.1–3 by considering the quantities relative to the photoproduct as equal to zero (i.e. $A_{tot}^{\lambda_{irr}/\lambda_{irr}}(\infty) = A_{PP}^{\lambda_{irr}/\lambda_{obs}}(\infty) = \varepsilon_{PP}^{\lambda_{irr}} = 0$). Therefore, Eqs. 1–3 can be considered as universal formulae applicable

to the photodegradation of any AB(1Φ) system at any non–isosbestic monochromatic irradiation wavelength irrespective of whether the photoproduct absorbs at that irradiation wavelength.

Nevertheless, the application of Eqs.1–3 was conditional to $F_{\infty}^{\lambda_{irr}}$ being higher than 1.2 (corresponding to $A_{PP}^{\lambda_{irr}/\lambda_{irr}}(\infty) < 0.65$) for the cases where both reactive species and photoproduct absorb, but in the absence of an excipient. This has proven to be a simple limitation as the former condition can easily be met by lowering the concentration of the initial species or possibly by reducing the path length of the irradiation ($l_{\lambda_{irr}}$). In the presence of an exogenous excipient molecule, the condition on *PP* ($A_{PP}^{\lambda_{irr}/\lambda_{irr}}(\infty) < 0.65$) holds with an additional limit on the highest absorbance that can be used for the excipient at the irradiation wavelength, $A_{Excip.}^{\lambda_{irr}} < 2.5$; a value that is generally beyond the linearity range of most organic molecules (3).

The formulation of the photokinetic factor (Eq.3) indicates that its value decreases with increasing total absorbance of the medium at the irradiation wavelength. As a consequence, the increase of $A_{tot}^{\lambda_{irr}/\lambda_{irr}}(\infty)$ induces a decrease in the overall photodegradation rate–constant.

Another important parameter that may find use in the determination of the quantum yields and in actinometry is the rate–law for AB(1Φ) photoreactions at t = 0, namely the initial reaction velocity, expressed as

$$\nu_{0,j}^{\lambda_{irr,i}/\lambda_{obs}} = \left(\varepsilon_{PP}^{\lambda_{obs}} - \varepsilon_{NIS}^{\lambda_{obs}}\right) \times l_{\lambda_{obs}} \times \Phi_{NIS\rightarrow PP}^{\lambda_{irr}} \times \varepsilon_{NIS}^{\lambda_{irr}} \times l_{\lambda_{irr}} \times F_0^{\lambda_{irr}} \times C_0 \times P_{\lambda_{irr}}$$

$$= \delta_{\lambda_{irr}} \times P_{\lambda_{irr}} \quad (4)$$

with $F_0^{\lambda_{irr}}$ being the photokinetic factor at t = 0 and $\delta_{\lambda_{irr}}$ a proportionality factor.

3.2. Integrated rate–law equations for isosbestic irradiation

The equations presented above were set for non–isosbestic irradiation exclusively because the semi-empirical modelling was based on a formula derived for non–isosbestic irradiation. Also, because the semi-empirical Eq.1 has not been derived by a closed–form integration, its formulation is incomplete and does not apply for all situations as suggested by the limitations on the absorbance values of the medium (e.g. $F_{\infty}^{\lambda_{irr}} < 1.2$). This is also evident for isosbestic irradiation (λ_{isos}) as the logarithmic formula (Eq.1) is not at all defined for isosbestic conditions, (since the denominator $A_{NIS}^{\lambda_{isos}/\lambda_{isos}}(0) - A_{PP}^{\lambda_{isos}/\lambda_{isos}}(\infty) = 0$). Therefore, a set of equations needs to be derived for this situation even though only a few isosbetic points usually exist on the spectra.

The invariance of the absorbance at the irradiation wavelength at an isosbestic irradiation, leading to a constant photokinetic factor throughout the reaction time, renders integration of this system's differential equation possible (16). Hence, the kinetics obeys a monoexponential integrated rate–law, given by

$$A_{tot}^{\lambda_{isos}/\lambda_{obs}}(t) = A_{tot}^{\lambda_{isos}/\lambda_{obs}}(0) + \left(A_{tot}^{\lambda_{isos}/\lambda_{obs}}(0) - A_{tot}^{\lambda_{isos}/\lambda_{obs}}(\infty)\right) \times \left(e^{-k_{NIS}^{\lambda_{isos}} \times t} - 1\right) \quad (5)$$

With its overall reaction rate–constant expressed as

$$k_{NIS,PP}^{\lambda_{isos}} = \Phi_{NIS\rightarrow PP}^{\lambda_{isos}} \times \varepsilon_{NIS}^{\lambda_{isos}} \times l_{\lambda_{isos}} \times P_{\lambda_{isos}} \times F_{\lambda_{isos}} \quad (6)$$

The reaction initial velocity for isosbestic conditions has the same formula as Eq.4 but with λ_{isos} being replaced by λ_{irr}.

4. Results and discussion

4.1. Photodegradation of NIS

The absorbance spectrum of *NIS* in ethanol is characterised by two main absorption 200–250 and 300–420 nm regions, spanning the UVB, UVA and part of the visible spectral ranges (Fig. 1). The main peak maxima for *NIS* in ethanol are located at 238 and 340 nm with the former having a much higher absorbance than the latter broader peak. *NIS* spectrum may be interpreted by the contribution of the independent absorptions of the nitrobenzene and the dihydropyridine chromophores. The long wavelength band (300–420 nm) belongs exclusively to the latter molecular moiety, whereas both chromophores input the UVB transition (17).

The photodegradation of *NIS* is easily evidenced by a change in the UV spectrum of the solution (Fig. 1). Exposure of ethanolic solutions of *NIS* to monochromatic irradiation results in the gradual increase of the absorbance regions of 200–230 nm and 260–320 nm with a peak appearing in the

latter region at 280 and a shoulder at 314 nm. A decrease in absorbance is also observed between 230 and 260 nm and 320–420 nm, with the appearance of three isosbestic points at 232, 259 and 320 nm. The region between 390–420 nm represents an exclusive absorption region for *NIS* as the spectrum of *PP* ends at *ca.* 370 nm. The timely evolution of the spectra and the simultaneous formation of identifiable isosbestic points suggest that the photoreaction proceeds smoothly without formation of by–products. Moreover, the irradiation of the *PP* (that was formed from *NIS*) at various wavelengths did not result in further spectral changes, indicating that the *PP* is photostable.

The hypsochromic shift observed in the absorption range 320–420 nm has been assigned to the $\pi \rightarrow \pi^*$ electronic transition in the dihydropyridine ring, while the hyperchromic effect in the 259-320 nm range is ascribed to the $\pi \rightarrow \pi^*$ electronic transitions in the aromatic ring (11). The latter may also involve an underlying $\pi \rightarrow \pi^*$ transition of the dihydropyridine in agreement with the spectral contribution of each chromophore to the overall *NIS* electronic spectrum (17).

The primary photoprocess of *NIS* photodegradation is the occurrence of an intramolecular electron transfer from the dihydropyridine to the nitrophenyl group leading to a radical ion pair (14,18). The favourable pathway for the decay of the latter intermediate involves a proton transfer followed by the elimination of a water molecule to produce the primary photoproduct (*PP*, Scheme 1) (14,19). The spatial proximity of the oxygen atom of the ortho-nitro group on the phenyl ring to the hydrogen atom of the non–coplanar dihydropyridine moiety favours the proton transfer which represents a key step in the phototransformation of *NIS* (14,19,20).

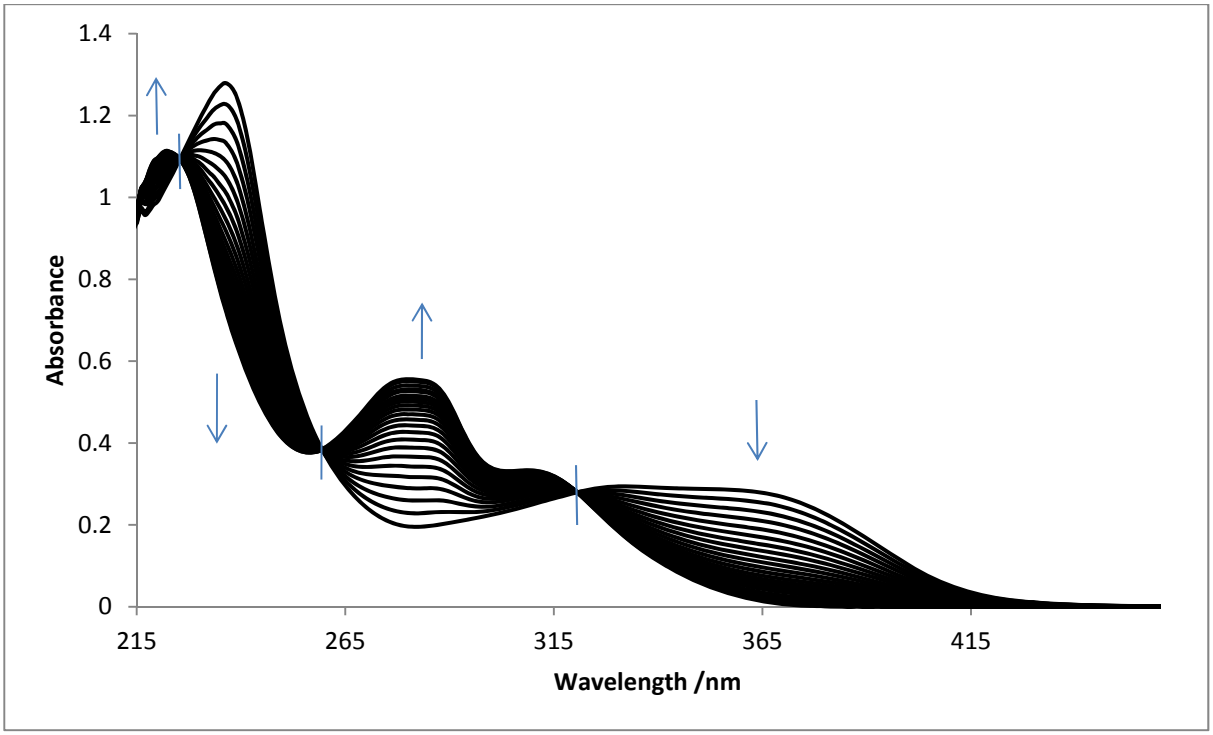

Fig. 1: Evolution of the electronic absorption spectra of 5.88 x 10^{-5} M *NIS* in ethanol subjected to a continuous irradiation with a 390 nm monochromatic beam (total irradiation time 2000 s at a radiant power of P_{390} = 7.76 x 10^{-7} einstein.s^{-1}.dm^{-3}). The arrows indicate the direction of the peaks' evolution during the photoreaction and the vertical lines cross the spectra at the isosbestic points (232, 259 and 320 nm).

4.2. Modelling NIS photodegradation kinetics

NIS photodegradation kinetics was studied by exposing freshly prepared ethanolic solutions to different irradiation wavelengths (λ_{irr} = 259, 281, 320, 345, 370, 380 and 390 nm) spanning different regions of its absorption spectrum including its isosbestic points (259 and 320 nm).

The variation of absorbance over time for each irradiation wavelength was recorded at a unique observation wavelength (λ_{obs} = 390 nm). These traces were labelled by their irradiation/observation wavelengths ($\lambda_{irr}/\lambda_{obs}$). Subsequently, the fitting of the experimental traces was conducted using

301 the suitable model equation (i.e. Eqs. 1 or 5 for non–isobestic and isosbetic irradiations,
302 respectively) (Fig. 2).

303

304 All the experimental traces were well fitted by the appropriate equation, thus confirming that (i)–
305 the mechanism of *NIS* involves a unimolecular photoreaction as set out in Scheme 1, (ii)– *NIS*
306 photodegradation obeys a Φ–order kinetics, and (iii) – the model equation (Eq.1) is valid in
307 describing AB(1Φ) photoreactions kinetics at any non–isosbestic and monochromatic irradiation.
308 Furthermore, a faster degradation was observed upon exposure to irradiation wavelengths in the
309 340–390 nm region compared to irradiations in the 235–320 nm region of the spectrum. This might
310 suggest that *NIS* photodegradation causative spectral range spans the UVA/visible regions.
311 However, since various experimental, spectroscopic and reactants' parameters are involved in the
312 equation of *NIS* photoreaction rate–constant (Eq.2), the former conclusion must be considered with
313 caution.

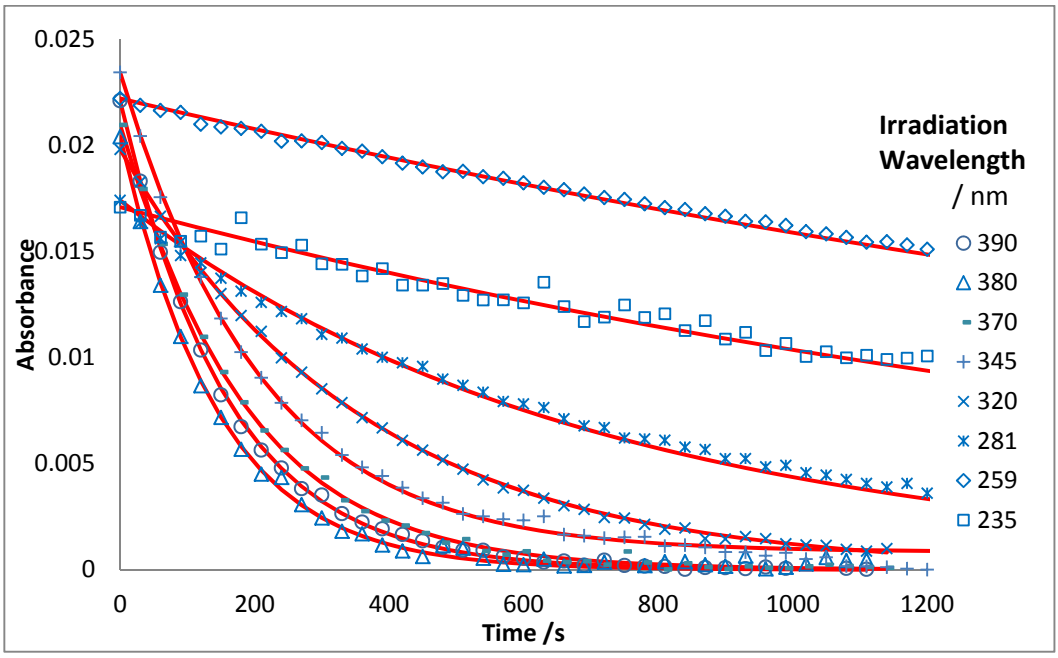

314

315 **Fig. 2:** The photokinetic traces of *NIS* in ethanol (7.84x 10^{-6} M) at λ_{irr}= 235, 259, 281, 320, 345,
316 370, 380 and 390 nm and observed at λ_{obs}= 390nm. The symbols represent the experimental data
317 while the lines represent the model fitted traces using the appropriate model equation.

4.3. Wavelength effects on NIS quantum yield

Fitting the models to the kinetic traces allows the determination of the respective value of $k_{NIS}^{\lambda_{irr}}$, which together with its formula (Eqs. 2 or 6) and data from the experimental kinetic traces (Fig.2), allows to readily determine the quantum yield values of *NIS* photodegradation at any monochromatic irradiation (Table 1).

Table 1: Quantum yields and reaction parameter values for the photodegradation of *NIS* under different monochromatic irradiation wavelengths.

$\boldsymbol{\lambda_{irr}}$ / nm	$\boldsymbol{A_{NIS}^{\lambda irr/390}(0)}$	$\boldsymbol{P_{\lambda irr}}$ /einstein.s^{-1}dm^{-3}	$\boldsymbol{k_{NIS}^{\lambda_{irr}}}$ **x 10^{3}** /s^{-1}	$\boldsymbol{\Phi_{NIS\rightarrow PP}^{\lambda_{irr}}}$
235	0.0171	8.64 x 10^{-7}	0.500	0.0041±0.0001
259	0.0222	2.64 x 10^{-7}	0.335	0.028±0.0111
281	0.0174	4.98 x 10^{-7}	1.240	0.122±0.0085
320	0.0198	3.53 x 10^{-7}	2.800	0.304±0.0157
345	0.0235	5.99 x 10^{-7}	5.100	0.326±0.0088
370	0.0210	6.32 x 10^{-7}	5.700	0.334±0.0200
380	0.0204	8.04 x 10^{-7}	7.300	0.345±0.0179
390	0.0221	1.02 x 10^{-6}	6.500	0.351±0.0069

The quantum yield of *NIS* photodegradation increases by more than 85 times with increasing wavelength from 235 to 390 nm (Table 1). Its values are more significant (> 0.1) for wavelengths higher than 280 nm. It is, however, clear that the electronic transition situated in the 320–390 nm

region is responsible for the highest phototransformation of *NIS* ($\Phi_{NIS\rightarrow PP}^{\lambda_{irr}} > 0.3$). The present values of $\Phi_{NIS\rightarrow PP}^{\lambda_{irr}}$ may suggest that the lowest singlet–state of the molecule is much more efficient in the photoconversion of *NIS* than are the other higher excited states, which underlines the important contribution of the $\pi\rightarrow\pi^*$ electronic transition of the dihydropyridine ring in the photochemistry of *NIS*.

Our $\Phi_{NIS\rightarrow PP}^{\lambda_{irr}}$ values agree with those reported in literature for *NIS* in methanol as 0.35 at λ_{irr} = 366 nm (14) and λ_{irr} = 365 nm (11). However, our $\Phi_{NIS\rightarrow PP}^{259}$ is more than 10–fold lower than the reported value ($\Phi_{NIS\rightarrow PP}^{\lambda_{irr}}$ = 0.25) for λ_{irr} = 254 nm (14). This discrepancy might be due to the large bandwidth of the filtered irradiation beam (i.e. a polychromatic light) used for the latter study which can only lead to average quantum yield values. The effect of the polychromatic irradiation beam which is clearly much more pronounced at 254 nm than at 366 nm, might be explained by a steeper variation of *NIS* quantum yield values in the 250–300 nm than in the 350–390 nm region (Table 1 and Fig.3). However, the $\Phi_{NIS\rightarrow PP}^{\lambda_{irr}}$ obtained in the present study match well the overall wavelength variation of the quantum yields observed for a *NIS* analogue, nifedipine (3). Incidentally, the similarity between *NIS* and nifedipine results indicate that the extension of the alkyl chain (*R*) on the ester (–COO–R) group (a methyl in nifedipine) does not significantly affect the photochemical efficiency of the main structural dihydropyridine–phenyl backbone. Also, the presence of the nitro group at the ortho position of the aromatic ring in some dihydrpyridine members such as *NIS* and nifedipine renders such molecules more prone to photolability as suggested by the relatively high quantum yields recorded for both molecules compared to those reported for other dihydropyridine members (21). In any case, $\Phi_{NIS\rightarrow PP}^{\lambda_{irr}}$ values indicate that the UVA and the earliest section of the visible region are most efficient in *NIS* photodegradation. From a more general view point, our findings on the quantum yield dependence on irradiation wavelength

as it has been observed for *NIS*, nifedipine (3), montelukast (5), fluvoxamine (6) and sunitinib (7) strongly underline the necessity of using monochromatic light for the determination of reliable values of quantum yields.

Besides, our *NIS* photodegradation quantum yields are well correlated with the irradiation wavelength (Fig. 3) via a well-defined sigmoidal pattern (Eq.7). A good agreement is found between experimental and calculated (Eq.7) values of the quantum yields (as indicated by the linear relationship in the inset of Fig.3). Therefore, the sigmoid equation may be found useful to estimate the quantum yield absolute values at any irradiation wavelength between 235 and 390 nm.

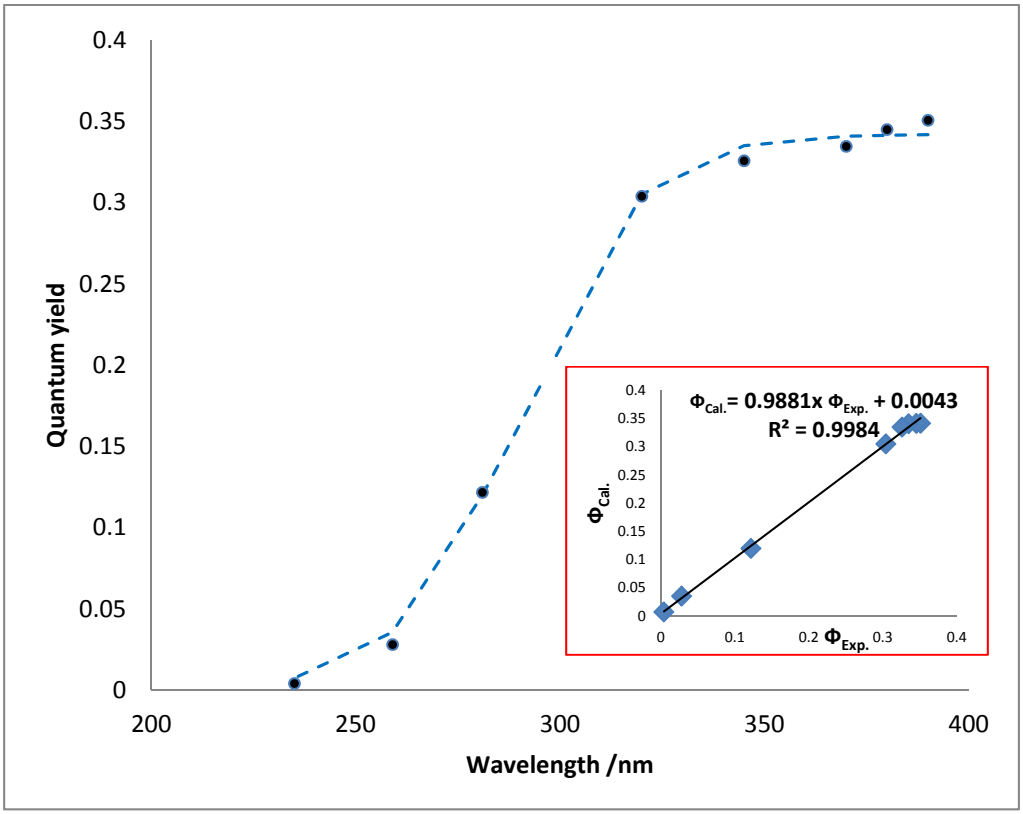

Fig. 3: Sigmoid-like pattern of *NIS* photodegradaion quantum yield values with irradiation wavelength. Inset: experimental ($\Phi_{\text{Exp.}}^{\lambda_{\text{irr}}}$) versus calculated ($\Phi_{\text{Cal.}}^{\lambda_{\text{irr}}}$) quantum yield values.

$$\Phi_{NIS\rightarrow PP}^{\lambda_{irr}} = \frac{0.26}{0.76 + 50 \times e^{-0.07(\lambda_{irr}-230)}} \quad (7)$$

370

371

372

373 *4.4. NIS* initial concentration effect on its photodegradation

374

375 Various concentrations of *NIS* in ethanol were selected within *NIS* linearity range (3.92 x 10^{-6} M to
376 1.58 x 10^{-4} M) to investigate their effect on *NIS* photodegradation rate. This was performed by
377 subjecting each freshly prepared solution to a particular irradiation wavelengths (λ_{irr} = 320, 350 or
378 390 nm), monitoring the absorbance at λ_{obs} = 390 nm and maintaining the radiant power
379 unchanged for the whole set of experiments realised for any given λ_{irr}.

380

381 The kinetic profiles and the determined overall rate–constants are presented in Table 2 and Fig.4.
382 The model equation fits well the traces with a 20 % decrease of the $k_{NIS}^{\lambda_{irr}}$ values observed for a 5–
383 fold increase in initial concentration for irradiation 320 and 350 nm whereas less than
384 6 % variation was recorded for an 8–fold increase of *NIS* initial concentration at λ_{irr} = 390 nm.

385

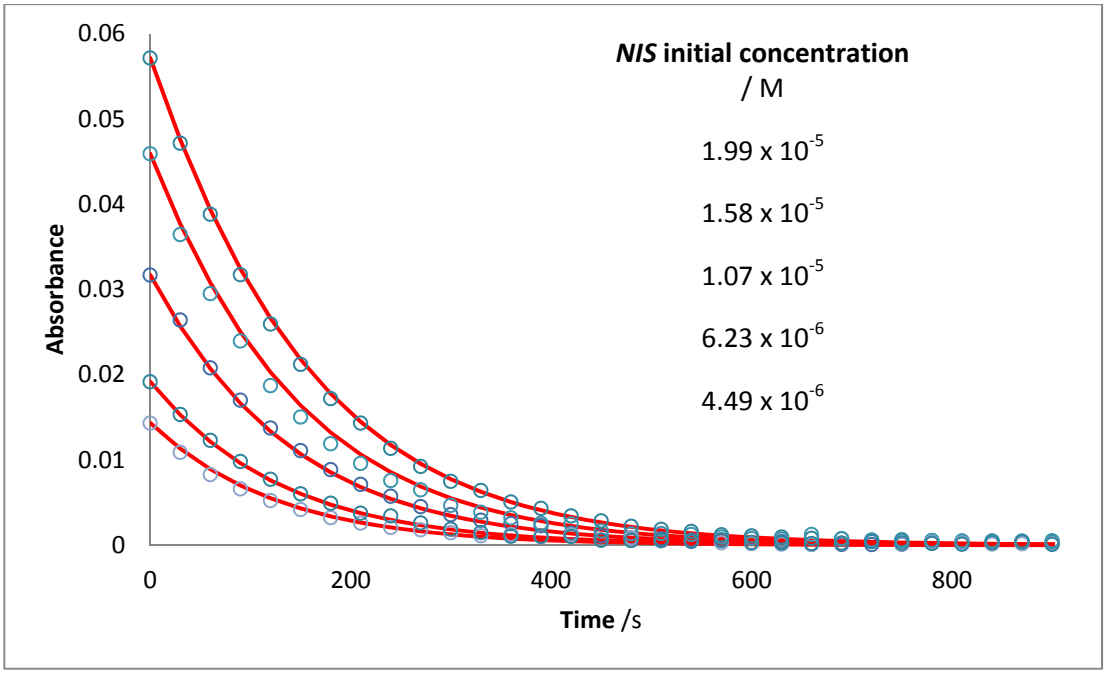

386

387 **Fig.4:** Photokinetic traces of *NIS* ethanolic solutions of various concentrations (4.49 x 10^{-6} –
388 1.99 x 10^{-5}) when irradiated at 350 nm and observed at 390 nm.

389 **Table 2**: Initial concentrations and overall rate–constants of *NIS* photodegradation measured at
390 various irradiation wavelengths.

λ_{irr}	$A_{NIS}^{\lambda_{irr}/390}(0)$	$k_{NIS}^{\lambda_{irr}}$ /s^{-1}	$C_{NIS}(0) \times 10^5$ /M
320	0.013	0.0043	0.396
	0.025	0.0041	0.826
	0.03	0.0039	1.01
	0.045	0.00375	1.53
	0.059	0.0035	2.06
350	0.014	0.0082	0.449
	0.019	0.0080	0.623
	0.032	0.0077	1.07
	0.046	0.0075	1.58
	0.057	0.0072	1.99
390	0.011	0.007	0.35
	0.022	0.007	0.73
	0.033	0.0069	1.12
	0.054	0.0069	1.86
	0.080	0.0066	2.81

391

The conditions imposed on the present experiments (as set out above and more specifically for non–isosbestic irradiations) meant that only the photokinetic factor's value within the rate–constant equation is affected by a change in the initial concentration (as all the other variables were kept unchanged between different experiments). As expected from the formulae of $F_{PP}^{\lambda_{irr}}$ and $k_{NIS}^{\lambda_{irr}}$ (Eqs.2 and 3), the higher *NIS* initial concentration the lower the $k_{NIS}^{\lambda_{irr}}$ value. Indeed, a linear relationship is established between these two factors for *NIS* for all non–isosbestic irradiations (320 and 350 nm) and/or initial concentration sets studied (Fig.5). The slight variation of $k_{NIS}^{\lambda_{irr}}$ with *NIS* concentration when the irradiation is performed at 390 nm, is also coherent with Eq.2 as the value of $F_{\infty}^{\lambda_{irr}}$ at the irradiation wavelength (390 nm, where only *NIS* absorbs) is constant for all the concentrations ($F_{\infty}^{\lambda_{irr}} = F_{PP}^{\lambda_{irr}} \approx 2.3$).

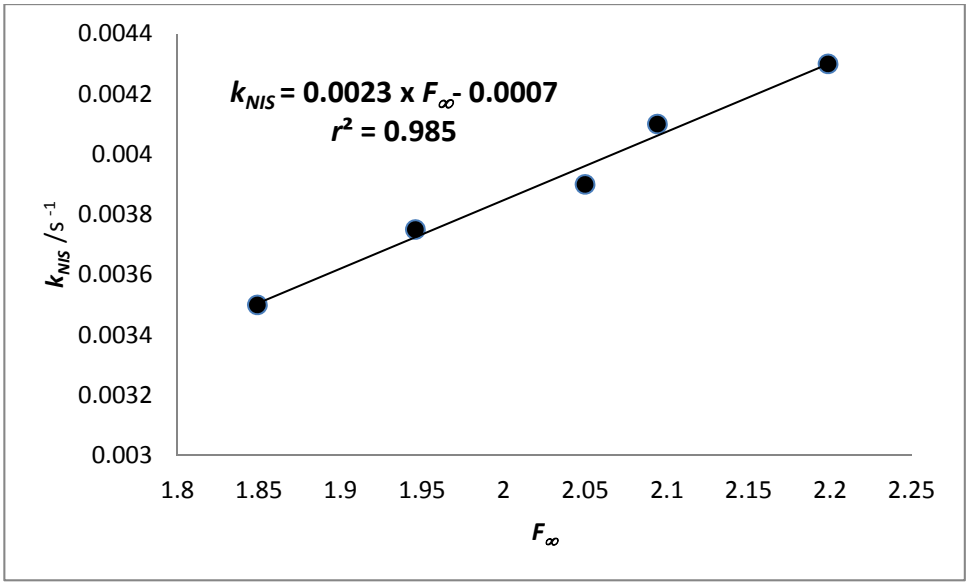

Fig.5: A Linear relationship between the overall rate–constant of *NIS* photodegradation (obtained as the fitting parameter of the kinetic data with Eq.1) and the photokinetic factor of the photoproduct (calculated using Eq.3) when irradiating various concentrations of *NIS* solutions (0.39–2.06 x 10^{-5} M) at 320 nm and observing at 390 nm.

411 The self-stabilization effect induced by the drug's initial concentration value, that works here for both
412 isosbestic and non–isosbetsic monochromatic–irradiation, would also be expected to hold for irradiation
413 with polychromatic light and can be postulated for drug mechanisms that involve more than a single
414 unimolecular photoreaction, AB(1Φ); (e.g. it has been proven for photoreversible reactions at any
415 irradiation wavelength (4), and for cyclic tri-molecular system involving up to six photochemical steps
416 when subjected to isosbestic irradiation (16).

417

418 The concept of photostabilisation through incrementation of the initial drug concentration, could in fact,
419 explain a number of experimental observations reported in the literature for many drugs (22,23). For
420 instance, the postulated change of reaction–order for *NIS* photodegradation kinetics, which was
421 attributed an apparent first–order kinetics for initial concentrations up to 3 x 10^{-5} M and a zero–order
422 kinetics for concentrations above 2 x 10^{-4} M (12), might be interpreted as a photoreaction slow down due
423 to increasing initial concentration. From the correlation line in Fig.6, a 2.75–fold reduction in $k_{NIS}^{\lambda_{irr}}$ can
424 be estimated to occur for the above concentrations. This would imply that the kinetic trace would have
425 been steeper for lower initial *NIS* concentrations than higher ones and therefore, might have justified the
426 fitting of the former with the exponential model of the first–order reaction and the latter with the linear
427 zero–order reaction model. A similar misinterpretation can, for instance, be made for *NIS* kinetic trace at
428 235 nm irradiation (Fig.2), which could be fitted with zero–order kinetics while the much steeper trace
429 resulting from irradiation at 390 nm (Fig.2) could be fitted with the first–order kinetics. This reiterates
430 the important need for an adequate kinetic elucidation of photodegradation reactions since obtaining a
431 good fitting with classical treatments, evidently cannot be informative enough to reach reasonable
432 conclusions on the relative reactivity of photodrugs.

433

A significant photostabilisation of *NIS* (and probably of many other drugs) can arguably be achieved by increasing its concentration, although this approach might considerably be limited by therapeutic dosages.

4.5. Quantification of *NIS* photostabilisation with excipient–dyes

Light absorption competitors have been proposed as a means to photostabilise photolibile drugs (22-26). Red–coloured iron oxides are employed in many solid (tablet) formulations for this purpose (22,27). In terms of interpretation, the reaction slowdown observed when increasing the concentrations of indigotine and azorubine, for instance, was construed as resulting from a decrease in *NIS* photodegradation quantum yield in methanolic solutions. The dyes were believed to act as quenchers of nisoldipine excited triplet–state as Stern–Volmer constructs had confirmed (11). The photodegradation rate–constant of nisoldipine in ethanol was also shown to decrease with increasing concentrations of β–carotene (15). These studies based their treatments on first–order kinetics and their conclusions were mainly reached by comparing the reactions rate–constant values. However, a comprehensive quantification of the effects of such light absorption competitors on the photoreaction overall rate–constant has not been, thus far, rationalised by a physicochemical/mathematical treatment. In our previous study (3), the reduction of the rate–constant could be directly linked to the concentration of the absorption–competitor using Φ–order kinetic equations. In the present study, the additives tatrazine (*TRZ*) and quinoline yellow (*QY*) have been studied as examples of excipient–dyes capable of retarding *NIS* photodegradation in ethanol.

458 *NIS* kinetic traces obtained in the presence of increasing concentrations of excipient–dyes (*TRZ* and
459 *QY*) were fitted with high accuracy to Eq.1 (Fig.6). Increasing the dyes concentrations was found to
460 be inversely proportional to the overall photodegradation rate–constant (Table 3).

461

462

463

464 **Table 3:** Dyes absorbance, overall reaction rate–constants, photokinetic factors, and percentage
465 reduction in reaction rates of *NIS* photodegradation in the presence of various concentrations of
466 *TRZ* and *QY* when irradiated and observed at 390 nm.

	$A_{dye}^{\lambda_{irr}}$ [a]	$F_{\infty}^{\lambda_{irr}}$	$k_{NIS}^{\lambda_{irr}}$ /s^{-1}	$\frac{k_{NIS}^{\lambda_{irr}}\left(A_{dye}^{\lambda_{irr}}=0\right)}{k_{NIS}^{\lambda_{irr}}\left(A_{dye}^{\lambda_{irr}}\neq 0\right)}$	% reduction [b]
NIS [c,d]	0	2.30	0.0080	1	0
Tartrazine (*TRZ*)	0.379	1.54	0.0052	1.54	35
	0.762	1.08	0.0039	2.05	51.25
	1.147	0.81	0.0032	2.50	60.00
	1.415	0.68	0.0022	3.64	72.5
Quinoline Yellow (*QY*)	0.261	1.73	0.0067	1.19	16.25
	0.472	1.40	0.0055	1.45	31.25
	0.792	1.06	0.0040	2.00	50
	1.137	0.82	0.0032	2.50	60

467 [a]: Absorbance of the dye measured at the irradiation wavelength of 390 nm for concentrations given
468 in Fig.7.
469 [b]: The constant concentration of *NIS* was 1.56 x 10^{-5} M.
470 [c]: The radiant power value for the experiments was P_{390} =1.74 x 10^{-6} – 1.78 x 10^{-6} einstein.dm^{-3}.s^{-1}.

471

472

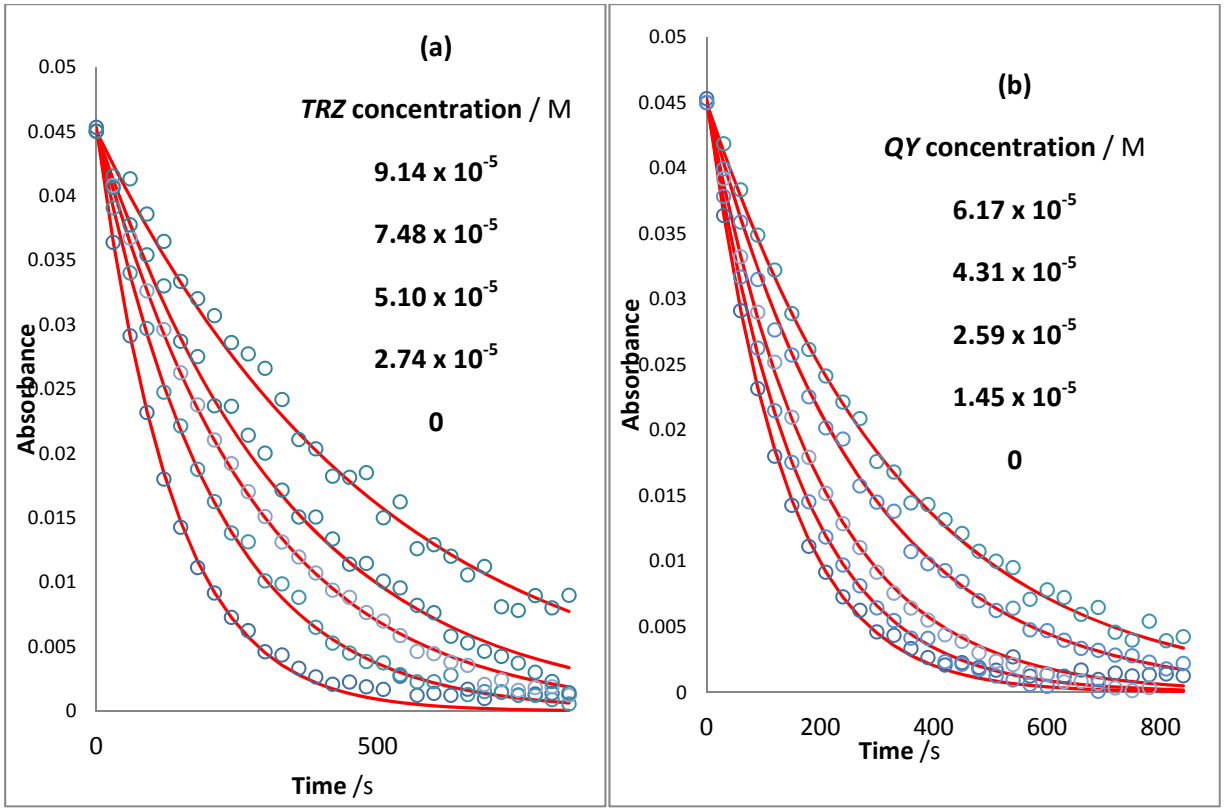

Fig.6: Effect of increasing (**a**) *TRZ* and (**b**) *QY* concentrations on the photodegradation traces of 1.56 x 10^{-5} M *NIS* solutions when irradiated and observed at 390 nm.

A good linear correlation is found between the values of the photokinetic factor ($F_{\infty}^{\lambda_{irr}}$) and the overall rate–constant ($k_{NIS}^{\lambda_{irr}}$) when the former is calculated by involving the values of the absorbances of the dyes in the expression of the medium's total absorbance as, $A_{tot}^{\lambda_{irr}/\lambda_{irr}}(\infty) = A_{PP}^{\lambda_{irr}/\lambda_{irr}}(\infty) + A_{Excip.}^{\lambda_{irr}}$ (Fig. 7, with $\lambda_{irr} = 390$ nm and $A_{PP}^{390/390}(\infty) = 0$). As a consequence, the higher the dye's absorbance, the smaller the $F_{\infty}^{\lambda_{irr}}$ value that leads to significant reduction of $k_{NIS}^{\lambda_{irr}}$ values (Fig.7, Table 3). Therefore, the true action of the light competitor on the photodegradation reaction is revealed in the reduction of the photokinetic factor value for increasing excipient–dye concentrations, but does not affect *NIS* quantum yield as might have been suggested (11).

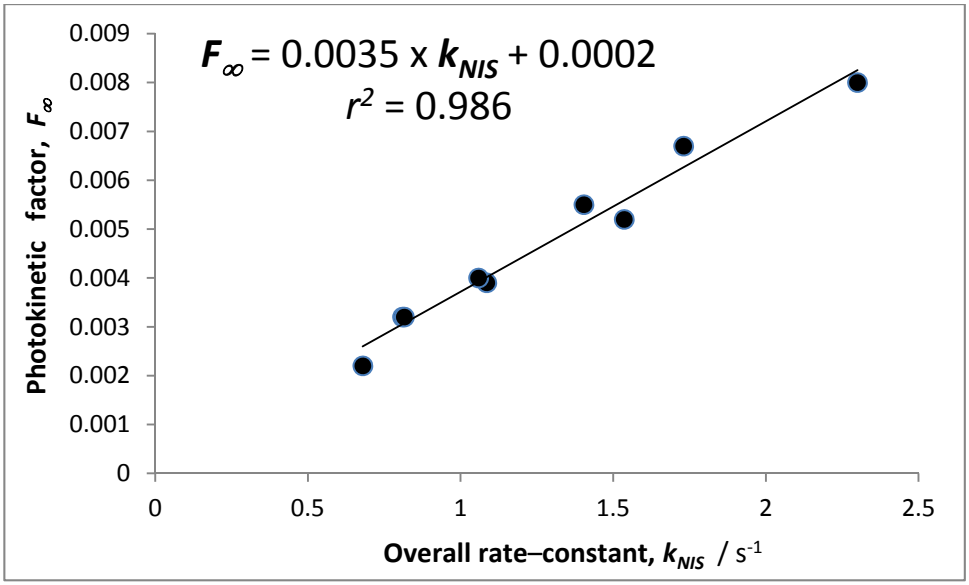

487

488 **Fig.7:** Linear relationship between $F_\infty^{\lambda_{irr}}$ and $k_{NIS}^{\lambda_{irr}}$ for data collected for both *TRZ* and *QY* various
489 concentrations (Table 3) in the presence of 1.56 x 10^{-5} M *NIS* irradiated and observed at 390 nm.

490

491

492 *4.6. NIS* actinometric potential

493

494 The ICH recommended quinine hydrochrolide actinometer for photostability testing purposes (8)
495 has been found to suffer from a number of limitations, including but not limited to an ill–defined
496 photochemical mechanism and a persistent thermal degradation in the dark (28). These drawbacks
497 seriously hamper the reliability of this actinometer. It is also noticeable that quinine hydrochrolide
498 has rarely been employed for the investigations of drugs' photodegradation in solution (22,29,30).
499 Nevertheless, no alternative actinometers have thus far been proposed. In this respect, the equations
500 for Φ–order kinetics have enabled the development of new AB(1Φ) actinometers including
501 conventional drug molecules (2,3,5-7).

502

Accordingly, the usefulness of *NIS* for actinometry was established by selecting four (i = 4) irradiation wavelengths (320, 345, 370 and 390 nm) within the region of fast photodegradation. For each wavelength, a set of "j" different radiant power values (spanning our instrumentation capacities) were performed on separate *NIS* solutions of the same concentration. The resulting traces were well fitted by Eq.1 (Fig.8), which then allowed the values of $k_{NIS,j}^{\lambda_{irr,i}}$ to be determined for each trace ($\lambda_{irr,i}$, $P_{\lambda_{irr,i}}^{j}$).

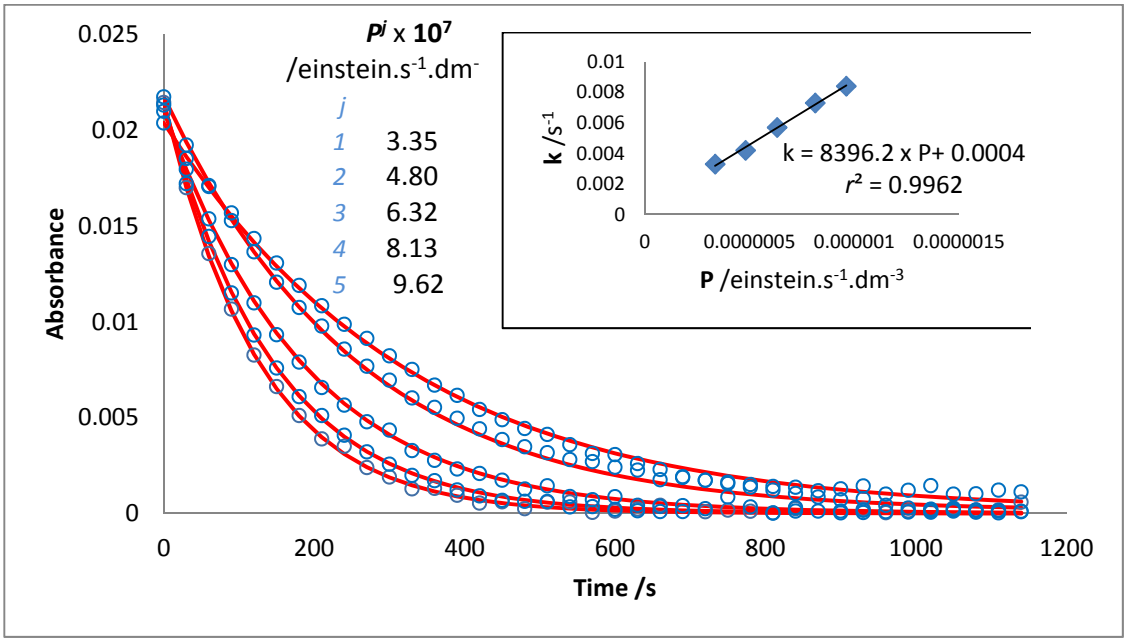

Fig. 8: Effect of increasing radiant power, P_{370}^{j} , on *NIS* kinetic traces 370/390. The circles represent the experimental traces and the lines represent the fitting traces using Eq.1. Inset: Correlation between $k_{NIS,j}^{\lambda_{irr,i}}$ of each kinetic trace and its corresponding P_{370}^{j}.

Increasing the radiant power at any irradiation wavelength had the effect of accelerating the rate of the photoreaction. As predicted by Eq.2, good linear correlations were found between $k_{NIS,j}^{\lambda_{irr,i}}$ and the corresponding $P_{\lambda_{irr,i}}^{j}$ values (Fig.9 and Table 4), with intercepts approaching a zero value and

519 **Table 4:** Correlation equations for the variation of *NIS* photodegradation overall rate–constants
520 ($k_{NIS}^{\lambda_{irr}}$) and initial reaction velocities ($v_0^{\lambda_{irr}/\lambda_{obs}}$) with radiant power ($P_{\lambda_{irr}}$), the corresponding $\beta_{\lambda_{irr}}$
521 and $\delta_{\lambda_{irr}}$ factors, and the span of radiant power employed for various monochromatic irradiations.

Irradiation wavelength $\boldsymbol{\lambda_{irr}}$ / nm	**Equation of the line** [a]	**Correlation coefficient,** $\boldsymbol{r^2}$	$\boldsymbol{P_{\lambda_{irr}} \times 10^7}$ /einst.s^{-1}.dm^{-3}
	$\boldsymbol{k_{NIS}^{\lambda_{irr}} = \beta_{\lambda_{irr}} \times P_{\lambda_{irr}} + intercept}$		
390	7902.7 x P_{390} - 5x10^{-6}	0.996	3.81 – 10.9
370	8850.8 x P_{370} + 5x10^{-7}	0.999	5.55 – 11.9
345	8391.1 x P_{345} - 7x10^{-6}	0.998	2.42 – 7.20
320	7558.4 x P_{320}+ 2x10^{-5}	0.996	1.34 – 4.35
	$\boldsymbol{v_0^{\lambda_{irr}/\lambda_{obs}} = \delta_{\lambda_{irr}} \times P_{\lambda_{irr}} + intercept}$		
390	- 197.98 x P_{390} - 5x10^{-6}	0.944	3.81 – 10.9
370	- 226.05 x P_{370} + 7x10^{-5}	0.956	5.55 – 11.9
345	- 124 x P_{345} - 1x10^{-5}	0.984	2.42 – 7.20
320	- 130.26 x P_{320} - 4x10^{-6}	0.996	1.34 – 4.35

522 [a] $k_{NIS}^{\lambda_{irr}}$, $v_0^{\lambda_{irr}/\lambda_{obs}}$ and intercepts expressed in s^{-1}; $\beta_{\lambda_{irr}}$ and $\delta_{\lambda_{irr}}$ in einst^{-1}.dm^3.

523

524 correlation coefficients of almost unity. The gradient of the equation was expressed as a factor
525 $\beta_{\lambda_{irr}}$(Eq.2).

526

527 In general, such linear relationships are expected to be found irrespective of *NIS* initial
528 concentration (as long as $A_{PP}^{\lambda_{irr}/\lambda_{irr}}(\infty) < 0.65$), and/or the radiant power value (that can be a
529 million–fold higher than $P_{\lambda_{irr.i}}^{j}$ used in this study (3)).

530 It is also interesting to notice that from an application viewpoint, the variation of $k_{NIS,j}^{\lambda_{irr,i}}$ with $P_{\lambda_{irr.i}}^{j}$
531 can be investigated independently of and prior to knowing the quantum yield of the AB(1Φ) system
532 at hand. This represents an advantage in developing new drug–actinometers.

533

Furthermore, the actinometric study can be even simpler to carry out if instead of using $k_{NIS,j}^{\lambda_{irr,i}}$ as a dependent variable, the initial reaction–rate ($v_{0,j}^{\lambda_{irr,i}/\lambda_{obs}}$, Eq.4) is employed. Indeed, the values of $v_{0,j}^{\lambda_{irr,i}/\lambda_{obs}}$ for the j radiant power experiments for the i^{th} irradiation wavelength can readily be obtained as the gradients ($\delta_{\lambda_{irr}}$) of the linear relationships fitting the very first experimental points of each photodegradation trace (Table 4, Fig.8). Obviously, the determination of the $\delta_{\lambda_{irr}}$ values for AB(1Φ) systems does not require the prior knowledge of both reaction attributes' and experimental parameters' values, and/or a complete trace. It is worth noting that $\delta_{\lambda_{irr}}$ and $\beta_{\lambda_{irr}}$ factors express different quantities (Eqs. 2 and 4) and hence do not directly correlate with each other.

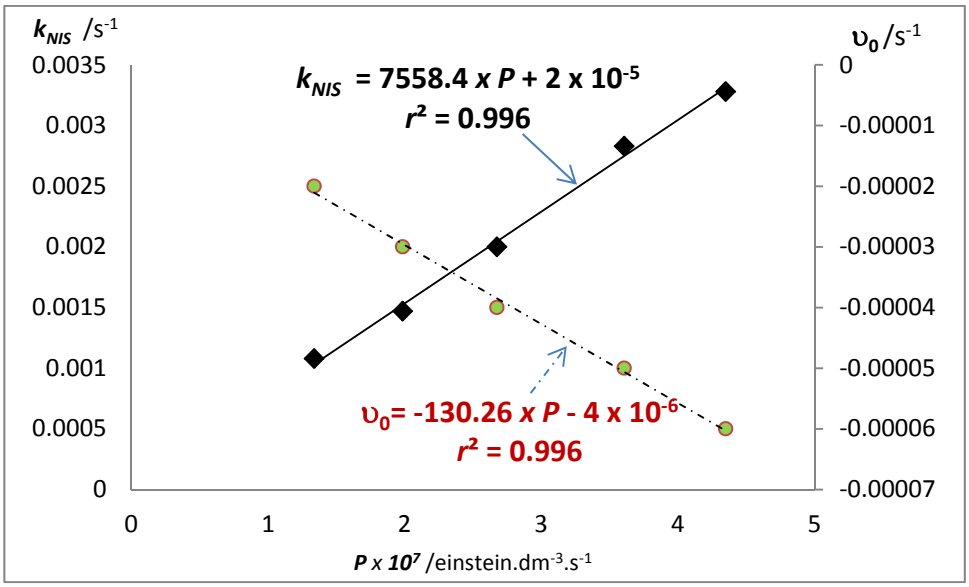

Fig. 9: Linear correlations between the parameters of the traces $k_{NIS,j}^{320}$ and $v_{0,j}^{320/390}$ against the radiant power, P_{320}^{j} for *NIS* in ethanol. The irradiation/observation wavelengths were 320/390, and the *j* values of the radiant power were taken from Table 4.

The values of the gradients ($\beta_{\lambda_{irr}}$ or $\delta_{\lambda_{irr}}$) offer the possibility of determining the radiant power value of any monochromatic irradiation beam between 320 and 400 nm, by proceeding as follows : (*a*)– irradiate *NIS* (or any AB(1Φ) system) at the selected wavelength and subsequently (*b*)–

551 determine either its rate–constant (by fitting the semi–empirical integrated rate–law model, Eq.1) or
552 determining its initial rate of photoreaction. The corresponding value of $\beta_{\lambda_{irr}}$, (*c*)– is worked out
553 from one of the linear equations set out in Fig.10 and (*d*)– the appropriate equation (for either $k_{NIS}^{\lambda_{irr}}$
554 or $v_{0(i,j)}^{\lambda_{irr}/\lambda_{obs}}$), Eq.8, can then be used to determine the value of the radiant power $P_{\lambda_{irr}}$ of the light–
555 source at the selected wavelength (Eq.8 was written by ignoring the lines' intercepts which have
556 approximately zero values, Fig.9).

557

$$P_{\lambda_{irr}} = \frac{k_{NIS}^{\lambda_{irr}}}{\beta_{\lambda_{irr}}} = \frac{v_{0(i,j)}^{\lambda_{irr}/\lambda_{obs}}}{\delta_{\lambda_{irr}}} \qquad (8)$$

558

559 Eq.8 should apply for any experiment if *NIS* initial concentration and the irradiation path–length
560 are similar to the ones used in this study ($C_{NIS}(0) = 7$ x 10^{-6} M and $l_{irr} = 2$ cm). However, if
561 $C_{NIS}(0)$ is the same but $l_{irr,actual}$ is different, then a small adjustment must first be made before the
562 $\beta_{\lambda_{irr}}$ factor is used in Eq.8. Mainly, the value of *PP* absorbance at the end of the reaction as
563 measured for the actual reaction ($A_{PP}^{\lambda_{irr}/\lambda_{irr}}(\infty)$) will be used to calculate the photokinetic factor in
564 two different ways, $F_{\infty,actual}^{\lambda_{irr}}$ using the optical path length $l_{\lambda_{irr,actual}}$, and the correcting $F_{\infty,corr.}^{\lambda_{irr}}$
565 using the optical path length of our experiment, $l_{\lambda_{irr}} = 2\ cm$. Then the $\beta_{\lambda_{irr}}$ factor (Fig.10) should
566 be multiplied by the product ($F_{\infty,actual}^{\lambda_{irr}} \times l_{\lambda_{irr,actual}}$) and divided by the product ($2 \times F_{\infty,corr.}^{\lambda_{irr}}$).

567

568 Therefore, *NIS* could be used as an actinometer for monochromatic irradiations in the region of
569 320–400 nm. Our method circumvents the problems encountered with many actinometers (31,32)
570 including the currently ICH recommended quinine actinometry (8), as the factors influencing the

photoreaction of the actinometer (initial concentration, irradiation wavelength, absorption coefficient of the species, excitation and monitoring optical path lengths) are all involved in Eq.8. Overall, because our approach is easy–to–implement (especially through the treatment using the initial velocity), it may represent an interesting method for the development of additional new drug–actinometers. In fact, it has thus far allowed us to propose four new accurate actinometers covering the whole spectrum of light, namely; *NIS* (320-400 nm), nifedipine (280-400 nm) (3), montelukast (258 – 380 nm) (5), fluvoxamine (260 – 290 nm) (6), sunitinib (320-480) (7) and 1,2-bis[2-methylbenzo[b] thiophen-3,3,4,4,5,5-hexafluoro-1-cyclopentene, DAE, for the visible 405 – 570 nm region (2).

Furthermore, the above study is useful to shed light on some crucial aspects relating to photochemical reaction attributes. It is interesting to note that besides its utility in actinometry, $\beta_{\lambda_{irr}}$ also appears to be an important factor that reflects the rate of a particular photoreaction (6). It can be compared between different studies using the same molecule at the same initial concentrations. This is because, $\beta_{\lambda_{irr}}$ does not depend on the radiant power which is hard to replicate between different experiments and especially when different research groups use different irradiation equipments. As such, unlike the overall rate–constant which is dependent on $P_{\lambda_{irr}}$, $\beta_{\lambda_{irr}}$ can be used to compare the rate of photodegradation of a particular molecule in different laboratory settings as long as the experiments are conducted using the same solvent, initial concentration and irradiation wavelength (adjustment might be required when $l_{\lambda_{irr}} \neq 2$, as set out above). The $\beta_{\lambda_{irr}}$ factors might help solving the long–standing problem of comparing photodegradation results obtained in different conditions (22).

It becomes obvious from our results that the photodegradation causative range of the drug can neither be precisely defined on the basis of quantum yield nor on that of the overall rate–constant values. The former represents an absolute value of the efficiency of the photoreaction which does not depend on the reaction parameters such as the absorption coefficient of the photoproduct, whereas the latter depends on a combination of reactivity, reagents' and experimental parameters, whose values are mostly variable with wavelength, in addition to the fact that the magnitude of $P_{\lambda_{irr}}$ can also be arbitrarily set. Hence, for a given molecule the $\beta_{\lambda_{irr}}$ factor stands as a better criterion for the definition of the reaction performance than $\Phi_{NIS\rightarrow PP}^{\lambda_{\mathrm{irr}}}$ or $k_{NIS}^{\lambda_{irr}}$, if the reactions performed to determine the $\beta_{\lambda_{irr}}$ factors, were carried out with the same initial concentration of the drug. This stems from the fact that the $\beta_{\lambda_{irr}}$ factor, defined exclusively by the irradiation (not the observation) conditions, encompasses the contribution of the absorptivities of the reacting species, the efficiency of the photoreaction, the excitation optical path length, and the initial concentration, i.e., all basic parameters influencing the rate of the photoreaction (with the exception of the radiant power). Therefore, the variation of the $\beta_{\lambda_{irr}}$ factors with wavelength can provide an effective tool to set the real limits for the photodegradation causative range of the drug (Fig.9).

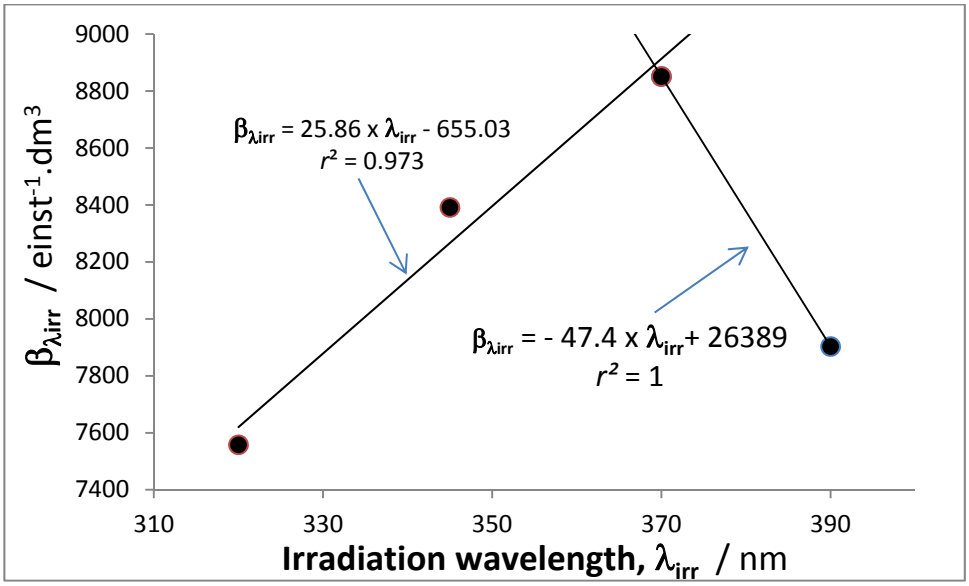

Fig. 10: Variation of $\beta_{\lambda_{irr}}$ factors with irradiation wavelengths (data from Table 4).

For *NIS*, the $\beta_{\lambda_{irr}}$ factors variation with irradiation wavelength follows a triangular pattern (Fig.10). Accordingly, *NIS* photoreaction is fastest under 370–nm irradiation, and its photodegradation causative range is situated between 320 and 400 nm (considering here that $\beta_{\lambda_{irr}} \geq 7400$ einstein^{-1}.dm^3).

5. Conclusion

The recently developed AB(1Φ) model has successfully been applied to describe the kinetics of *NIS* photodegradation. This model can describe the kinetics of any AB(1Φ) system much more accurately than the classical treatments based on thermal reaction orders. *NIS* quantum yields of photodegradation were found to follow a sigmoid like function with irradiation wavelength hence allowing the estimation of this parameter at any monochromatic irradiation wavelength in the 230–390 nm range. It has also become possible to quantify the self–stabilisation effect due to increasing the initial species concentration by a procedure using the rate–constant equation for AB(1Φ) systems. *NIS* photostabilisation by the presence of photostable excipient–dyes *TRZ* and *QY*, which act as absorption competitors as their electronic spectra overlap the same spectral range as *NIS*, has also been studied. Both species were shown to significantly reduce *NIS* photodegradation (up to 70%, for concentrations within the linearity ranges of these dyes). The observed photostabilising effect has also been successfully rationalised using the simple AB(1Φ) Φ–order kinetics equations which are capable of describing and predicting the effect of any photoabsorbing photostable species at the selected irradiation wavelength. Finally, it was shown how *NIS* may be used as a simple and accurate actinometer for monochromatic irradiations within the 320–400 nm spectral range. A new

633 approach of evaluating the photodegradation causative range is proposed on the basis of the
634 variation of $\beta_{\lambda_{irr}}$ factor values with wavelength.

635

636 These findings confirm the usefulness and flexibility of the kinetic equations, set out for
637 Φ–order photoreactions of the AB(1Φ) type, to investigate a number of aspects relating to drug
638 photodegradation, photostabilisation and actinometry.

639

640

641

642 **References**

643 (1) Maafi, M.; Brown, R. G. The kinetic model for AB(1Φ) systems. A Closed-form integration
644 of the differential equation with a variable photokinetic factor. *J. Photochem. Photobiol. A: Chem.*
645 **2007**, 187, 319-324.

646 (2) Maafi, M. The potential of AB(1Φ) systems for direct actinometry. Diarylethenes as
647 successful actimometers for the visible range. *Phys. Chem. Chem. Phys.* **2010** 12, 13248–13254.

648 (3) Maafi, W.; Maafi, M. Modelling nifedipine photodegradation, photostability and
649 actinometric properties. *Int. J. Pharm.* **2013**, 456 153-164.

650 (4) Maafi, M.; Maafi, W. Φ-order kinetics of photoreversible drug reactions. *Int. J. of Pharm.*
651 **2014**, 471, 536-543.

652 (5) Maafi, M.; Maafi, W. Montelukast photodegradation: Elucidation of Φ-order kinetics,
653 determination of quantum yields and application to actinometry. *Int. J. Pharm.* **2014**, 471, 544-552.

654 (6) Maafi, M.; Maafi, W. Quantitative assessment of photostability and photostabilisation of
655 Fluvoxamine and its design for actinomery. *Photochem. Photobiol. Sci.* 2015, 14, 982-994.

656 (7) Maafi, M.; Lee, L.Y. Actinometric and Φ–order photodegradation properties of anti-cancer
657 Sunitinib. *J. Pharm. Biomed. Anal.* 2015, 110, 34-41.

658 (8) ICH. Guidelines for industry Q1B photostability testing of new substances and products.
659 *Fed. Regist.* **1996**, 62, 27115-27122.

660 (9) Marinkovic, V.; Agbaba, D.; Karljikovic-Rajic, K.; Comor, J.; Zivanov-Stakic, D. UV
661 derivative spectrophotometric study of the photochemical degradation of nisoldipine. *Il Farmaco*
662 **2000**, 55, 128–133.

(10) Alvarez-Lueje, A.; Naranjo, L.; Nunez-Vergara, L. J.; Squella, J. A. Electrochemical study of nisoldipine: analytical application in pharmaceutical forms and photodegradation. *J. Pharm. Biomed. Anal.* **1998**, 16, 853–862.

(11) Mielcarek, J.; Augustyniak, W.; Grobelny, P.; Nowacka, G. Photoprotection of 1,4-dihydropyridine derivatives by dyes. *Int. J. of Pharm.* **2005**, 304, 145–151.

(12) Huang, C.; Liu, H.; Ren, J.; Du, X. Studies of photodegradation stability of nisoldipine. *Chinese J. Pharm.* **1996**, 27, 26-27.

(13) Marinkovic, V.D.; Agbaba, D.; Karljikovic-Rajic, K.; Vladimirov, S.; Nedeljkovic, J.M. Photochemical degradation of solid-state nisoldipine monitored by HPLC. *J. Pharm. Biomed. Anal.* **2003**, 32, 929-935.

(14) Fasani, E.; Dondi, D.; Ricci, A.; Albini, A. Photochemistry of 4-(2-nitrophenyl)-1,4-dihydropyridines. Evidence for electron transfer and formation of an intermediate, Photochem. Photobiol. 82 (2006) 225-230.

(15) J. Mielcarek, P. Grobelny, P. Szamburska, The effect of beta-carotene on the photostability of nisoldipine. Methods Find. Exp. Clin. Pharmacol. 27 (2005) 167.

(16) M. Maafi, R.G. Brown, General analytical solutions for the kinetics of AB(k,Φ) and ABC(k,Φ) systems, Int. J. Chem. Kinet. 37 (2005) 162-174.

(17) A. Krufurst, J. Kuhan, Quantum chemical interpretation of electronic absorption spectra of the hantzsch dihydropyridines, Coll. Czech. Chem. Commun. 43 (1983) 1422-1428.

(18) F.M. Martens, J.W. Verhoeven, C.A.G.O. Varma, P. Bergwerf, photooxidation of 1,4-dihydropyridines by various electron acceptors: a laser flash photolysis study, J. Photochem., 22 (1983) 99-113.

685 (19) X.Q. Zhu, H.R. Li, Q. Li, T. Ai, J.Y. Lu, Y. Yang, J.P. Cheng, Detrmination of the C4-11
686 bond dissociation energies of NADH models and their radical cations in acetonitrile, Chem. Eur. J.
687 9 (2003) 871-880.

688 (20) M. Cotta-Ramusino, M.R. Vari, Force field and semi-empirical MO conformational analysis
689 of dihydropyridine calcium-channel antagonists, J. Mol. Struct. (Theochem.). 492 (1999) 257-268.

690 (21) E. Fasani, D. Dondi, A. Ricci, A. Albini, Photochemistry of Hantzsch 1,4-dihydropyridines
691 and pyridines, Tetrahedron. 64 (2008) 3190-3196.

692 (22) J.T. Piechocki, K. Thoma, Pharmaceutical Photostability and Photostabilisation
693 Technology, Informa Healthcare: London, 2010.

694 (23) H.H. Tonnesen, Photostability of Drugs and Drug Formulations, second ed., CRC Press:
695 London, 2004.

696 (24) R.C. Rowe, P.J. Sheskey, P.J. Weller, Handbook of pharmaceutical excipients, third ed.,
697 Pharmaceutical Press and American Pharmaceutical Association, 2003.

698 (25) Albini, A., and Fasani E., 1998. Drugs Photochemistry and Photostability. The Royal
699 Society of Chemistry: Cambridge.

700 (26) K. Thoma, R. Klimek, Photostabilization of drugs in dosage forms without protection from
701 packaging, Int. J. Pharm. 67 (1991) 169-175.

702 (27) D.S. Desai, M.A. Abdelnasser, B.A. Rubitski, S.A. Varia, Photostabilizaton of uncoated
703 tablets of sorivudine and nifedipine by incorporation of synthetic iron oxides, Inter. J. of Pharm.
704 103 (1994) 69-76.

(28) S.W. Baertschi, K.M. Alsante, H.H. Tonnesen, A critical assessment of the ICH guideline on photostability testing of new drug substances and products (Q1B): recommendation for revision, Journal of Pharmaceutical Sciences, 99 (2010) 2934-2940.

(29) C.A. De Azevedo Filho, D. De Filgueiras Gomes, J.P. De Melo Guedes, R. M. F. Batista, B.S. Santos, Considerations on the quinine actinometry calibration method used in photostability testing of pharmaceuticals, J. of Pharm. Biomed. Anal. 54 (2011) 886-888.

(30) S.W. Baertschi, Commentary on the quinine actinometry system described in the ICH draft guideline on photostability testing of new drug substances and products, Drug Stab. 1 (1997) 193-195.

(31) H.J. Kuhn, S.E. Braslavsky, R. Schmidt, Chemical actinometry (IUPAC Technical Report), Pure Appl. Chem. 76 (2004) 2105-2146.

(32) M. Montalti, A. Credi, L. Prodi, M.T. Gandolfi, Handbook of Photochemistry, third ed., CRC Press, USA, 2006.